Journal of the Serbian Chemical Society
JSCS-info@shd.org.rs • www.shd.org.rs/JSCS
J. Serb. Chem. Soc. *82* (3) 289–301 (2017)
JSCS–4966
UDC 54.06:546.34+546.27'171:
532.14:54.04:519.677
Original scientific paper

QTAIM investigations of decorated graphyne and boron nitride for Li detection

MARYAM DEHESTANI[1], LEILA ZEIDABADINEJAD[1,2]*
and SEDIGHEH POURESTARABADI[1,2]

[1]*Department of Chemistry, Shahid Bahonar University of Kerman, Kerman 76169, Iran and* [2]*Young Researchers Society, Shahid Bahonar University of Kerman, Kerman 76169, Iran*

(Received 25 July, revised 5 November, accepted 7 November 2016)

Abstract: The interactions between thirteen Li atoms and graphyne (GY) and boron nitride (BN-yne) were investigated by the density functional theory (DFT). The electronic and structural properties of the interactions between the hollow sites of GY and BN-yne with Li atoms were unveiled within the quantum theory of atoms in molecules (QTAIM) framework. Theoretical understanding of the interactions between Li atoms and extended carbon-based network structures is crucial for the development of new materials. Herein, calculations to explore the impact of Li decoration on the GY and BN-yne are reported. It was predicted that Li decoration would increase the density of state of these sheets. Owing to strong interactions between Li and the GY and BN-yne, dramatic changes in the electronic properties of the sheets together with large band gap variations have been observed. The present study sheds deep insight into the chemical properties of the novel carbon–based two-dimensional (2D) structures beyond the graphene sheet.

Keywords: graphyne; BN-yne; chemical property; density of state; DFT.

INTRODUCTION

Carbon, the element responsible for life on earth, has many unique properties brought about by its ability to form diverse sp, sp^2, and sp^3 bondings. In organic systems, carbon atoms form a variety of structures ranging from linear chain to square, pentagonal, and hexagonal rings. In molecules, such as coronene, five hexagonal rings of carbon (C) surround a pentagonal ring, resulting in a buckled structure. However, in condensed matter systems for a long time only two allotropes of carbon were known. In recent years, two-dimensional structures of carbon allotropes have become one of the most promising new materials for

* Corresponding author. E-mail: lzeidabadi@yahoo.com
doi: 10.2298/JSC160725012D

nanotechnology. Carbon-based materials, such as carbon nanotubes, graphene, and other graphitic carbon nanomaterials, have attracted particular attention because of their low cost, high electronic conductivity, and electrocatalytic activity.[1–3] Depending on their size and shape, these materials could be semiconducting or conducting, making them potentially useful for a wide range of applications. Much less effort has been devoted to the synthesis and characterization of sp-hybridized allotropes, such as quasi-one-dimensional (1D) poly-ynes[4–6] and two-dimensional (2D) graphynes and graphdynes.[7,8] Yet, many theoretical reports suggest that alkyne-based 2D materials could exhibit similar, or even better, charge mobility than the other allotropes. Beyond graphene, GY is another unnatural allotrope of carbon composed of sp and sp^2 mixed C atoms the atomic structure was which was first suggested by Baughman *et al.*[9] It is obtained by replacing one third of the carbon–carbon bonds in graphene with triple-bonded carbon linkages.[9] There are several studies on different properties of GY and its related structures in the literature.[10–15] Most of these works have mainly focused on the electronic structure of GY and its substructures. Based on the density functional theory (DFT) together with the Boltzmann transport Equation, Long *et al.*[12] revealed that graphdyne is a semiconductor with a band gap of 0.46 eV. Zhou *et al.*[13] investigated the nature of the bonding and energy band structure of GY and its BN analog, named ''BN-yne'' using the DFT within the generalized gradient approximation. Zhang *et al.*[14] studied the energetics and dynamics of Li in GY. They found that the high Li mobility and high storage capacity could make GY a promising candidate for the anode material in Li-ion battery applications.

In this paper, a theoretical study of the interaction between Li on GY and BN rings BN-yne is presented. These intermolecular interactions, to the best of our knowledge, have not been studied and presented in previous theoretical calculations. The stability and electronic properties of the resulting complexes were unveiled by means of various quantum chemical approaches. This should help to understand more thoroughly the origin of the intermolecular interactions on GY and BN-yne systems. Analyzing the nature of the interaction between Li and the GY and BN-yne systems provides a good basis for the development and support of a chemical model. Accordingly, in the present work, the nature and properties of the interactions between Li and the GY and BN-yne systems were deciphered in energetic, topological, MEP, and charge transfer analyses.

The main objective of this theoretical work concerned the achievement of valuable information on the stability of the GY and BN-yne systems and on the strength of the interactions of Li on the GY and BN-yne systems, which would be of importance for the mentioned applications.

METHODOLOGY

GY and BN-yne sheets consisting of 84 atoms were considered and end of their atoms were saturated with hydrogen atoms to reduce boundary effects. The optimization of GY, BN--yne, GY–Li and BN-yne–Li complexes, without any symmetry constraints, was realized at the B3LYP/6–31g(d) level of theory by means of the Gaussian 09 suite of programs.[16] The adsorption energies (E_{ad}) of Li atoms on GY and BN-yne were obtained using the following equation:

$$E_{ad} = E(\text{GY or BN-yne/Li}) - E(\text{GY or BN-yne}) - n\,E\,(\text{Li}) \quad (1)$$

where E (GY or BN-yne/Li) is the energy of the GY or BN-yne complexes and E(Li) is the energy of an isolated Li atom and n is number of Li atoms. E(GY or BN-yne) is the optimized energy of GY or BN-yne, respectively. The negative value of E_{ad} indicates the exothermic nature of the adsorption. Topological analysis of the electron density of the DFT-optimized structures of the complexes between Li on GY and BN-yne was performed *via* the quantum theory of atoms in molecules (QTAIM).[17] The QTAIM analyses were concentrated on the B3LYP/6–31g (d) calculated wave function of the electron density obtained for the optimized structures. The resulting formatted wave function files were used as inputs to the AIM2000 program[18] for calculating topological properties of electron density and Laplacian. Considering the local virial theorem, the following characteristics of the bond critical point (BCP) were taken into account: electron density (ρ_c), its Laplacian ($\nabla^2_{\rho_c}$), the electronic kinetic energy density (G_c), the electronic potential energy density (V_c), and the total electronic energy density (H_c) at BCPs. These properties were chosen as the most useful indicators for quantitative representation of intra-atomic interactions in the coordination of complexes. A theoretical understanding of the reactivates (such as nucleophilicities and electrophilicities) of molecules was based on the frontier molecular orbitals (FMO) theory, developed by Fukui and co -workers.[19,20] An important aspect of this theory is the focus on the interactions of the lowest unoccupied and the highest occupied molecular orbitals (LUMO and HOMO). According to the FMO theory, a high value of the HOMO energy indicate a probable tendency of the molecule to give electrons to an appropriate acceptor molecule (an electrophilic species) and the LUMO energy indicates the ability of the molecule to accept electrons from a donor molecule (a nucleophilic species).

RESULTS AND DISCUSSION

Structure and stability of compound

The atomic structures of GY and BN-yne decorated with Li atoms are shown in Fig. 1. There are several attachment sites for Li atoms on GY and BN-yne, *i.e.*, on top of the C atoms and in the hollow sites of sp- and sp^2-bonded hexagons and sp-bonded triangles. According to the results obtained by Zhang and co-worker,[14] hollow sites are more stable than top sites. In the present work, the interaction of Li atoms on the hollow sites in GY and BN-yne were compared. The bond lengths in the structures of GY and BN-yne decorated with Li atoms are given in Table I. In the optimized configuration of GY, the bond lengths between two sp^2-hybridized carbon atoms (L1 and L5) are 1.40 and 1.41 Å, respectively, suggesting that the p–conjugate feature of GY is kept in the hexagons. The short distance between the sp-hybridized carbon atoms (L3 and L4) are 1.22

and 1.40 Å) in the chain indicates that a C≡C triple bond is formed between them. In the optimized BN-yne structure, the bonds between N and B (L1, L2, L6 and L7) with bond lengths 1.43, 1.4343, 1.47 and 1.47 Å, respectively, are sp^2--hybridized. The short distances between the sp-hybridized carbon atoms (L3 and L4) in the chain, 1.34 and 1.22 Å, respectively, indicate that N≡C and C≡C triple bonds are formed between them.

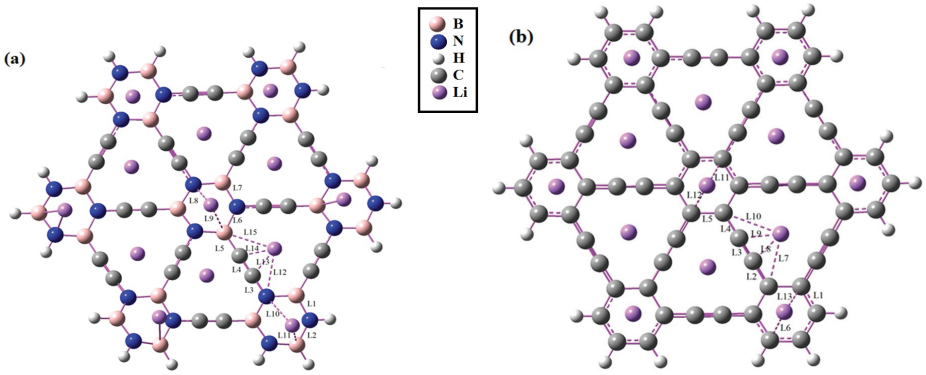

Fig. 1. The most stable structures of (a) BN-yne–Li and (b) GY–Li complexes in the gas phase.*

TABLE I. Selected bond length (l) for the GY, BN-yne, GY–Li and BN-yne–Li molecules

Molecule	l_{GY} / Å	$l_{GY–Li}$ / Å	l_{BN-yne} / Å	$l_{BN-yne–Li}$ / Å
L1	1.40	1.43	1.4327	1.46
L2	1.40	1.37	1.4343	1.46
L3	1.22	1.24	1.3357	1.31
L4	1.40	1.37	1.2232	1.24
L5	1.41	1.46	1.4787	1.45
L6		2.18	1.4680	1.50
L7		2.97	1.4680	1.48
L8		2.27		2.23
L9		2.27		2.25
L10		2.96		2.71
L11		2.20		2.16
L12		2.19		2.99
L13		2.22		2.29
L14				2.21
L15				2.95

Li adsorption on GY and BN-yne

The Li atoms were placed perpendicular to the GY and BN-yne surfaces above the center of the hollow sites. To investigate the changes in the electronic charge density considering GY and BN-yne caused by the physi- or chemi-sorp-

*For full color versions of the figures from this paper, please refer to its electronic version at web pages of the journal: http://shd.org.rs/jscs

tion of Li atoms, the charge transfer (*QT*) from the GY and BN-yne sheets to the Li atoms was calculated based on natural bond orbital (NBO) population schemes.[21] The *QT*, defined as the charge variation caused by Li adsorption, is a useful measure of the importance of the intermolecular orbital interaction between the sheets and Li atoms. As listed in Table II, the high charge transfer values from the corresponding sheets to Li atoms are an indicator of the acceptor character of the Li atoms. Table II shows that the direction of the charge transfer is determined by the relative position of the HOMO and LUMO of the adsorbate (Li atoms) with respect to the Fermi level in pure GY and BN-yne. If the LUMO of the adsorbate lies at a lower energy than the Fermi level of the sheets, electrons will flow from the sheets to the adsorbate, making the sheets p–type semiconductors. Adsorbates with the HOMO lying above the Fermi level of sheets act as donors and the sheets exhibits n–type semiconducting behavior. More detailed information about the simulation of the different Li–GY and Li–BN-yne systems; including values of E_{ad}, the energy of the highest occupied molecular orbital energy (E_{HOMO}), the lowest occupied molecular orbital energy (E_{LUMO}), the energy gap (E_g), the Fermi energy (E_F) and the *QT* for these configurations are listed in Table II. The negative *QT* and E_{ad} of Li on the sheets reveal the physical nature of the interaction.

TABLE II. Quantum molecular descriptors of GY, BN-yne, GY–Li and BN-yne–Li

	E_{HOMO}[a] / eV	E_{LUMO}[b] / eV	E_F[c] / eV	E_g[d] / eV	E_{ad}[e] / eV	*QT*[f]
BN-yne	–5.7797	–2.8272	–4.3048	2.9524		
BN-yne–Li_1	–3.0259	–2.6803	–2.8544	0.3456	–0.9932	–0.4555
BN-yne–Li_2	–2.8762	–2.5605	–2.7184	0.3156	–1.7578	–0.5139
BN-yne–Li_3	–2.8082	–2.5034	–2.6558	0.3048	–2.6966	–0.5342
BN-yne–Li_4	–2.7810	–2.4871	–2.6341	0.2939	–3.6762	–0.5445
BN-yne–Li_5	–2.8327	–2.7374	–2.7864	0.0952	–4.3891	–0.5507
GY	–5.4803	–3.9674	–4.7238	1.5129		
GY–Li_1	–5.2028	–4.0491	–4.6259	1.1537	–2.1088	–0.4604
GY–Li_2	–3.8749	–3.6898	–3.7824	0.3782	–4.3456	–0.5172
GY–Li_3	–3.7034	–3.6463	–3.6735	0.3210	–6.4137	–0.5366
GY–Li_4	–3.4939	–3.1728	–3.3334	0.1850	–8.6315	–0.5464
GY–Li_5	–3.5130	–3.1348	–3.3252	0.0571	–11.051	–0.5523

[a]Highest occupied molecular orbital energy (E_{HOMO}); [b]lowest occupied molecular orbital energy (E_{LUMO}); [c]Fermi energy (E_F); [d]gap energy (E_g); [e]adsorption energy (E_{ad}); [f]charge transfer (*QT*)

As a result, the transferred charge (0.4555) from GY to Li is remarkably more than that from BN-yne (0.4506). These data indicate that the Li atoms undergo physical adsorption on the sheets, thus, suggesting that GY and BN-yne may be suitable for detecting the presence of Li. The calculated density of states (*DOS*) plots (Fig. 2) show that the Li adsorption senses the electronic properties of the GY and BN-yne and hence, the E_g of the sheets was reduced –12.87 and

–21.34 eV, respectively, on addition of thirteen Li atoms to the hollow sites. However, the stability of these configurations could be explained by noting the fact that Li atoms have low electronegativity and a positive charge, and thus, a suitable p–cation interaction is formed between the Li atoms and the π electrons of the hollow sites. The local *DOS* plots confirm that when Li atoms are lying on GY and BN-yne, the Fermi levels of GY and BN-yne move to LUMO levels.

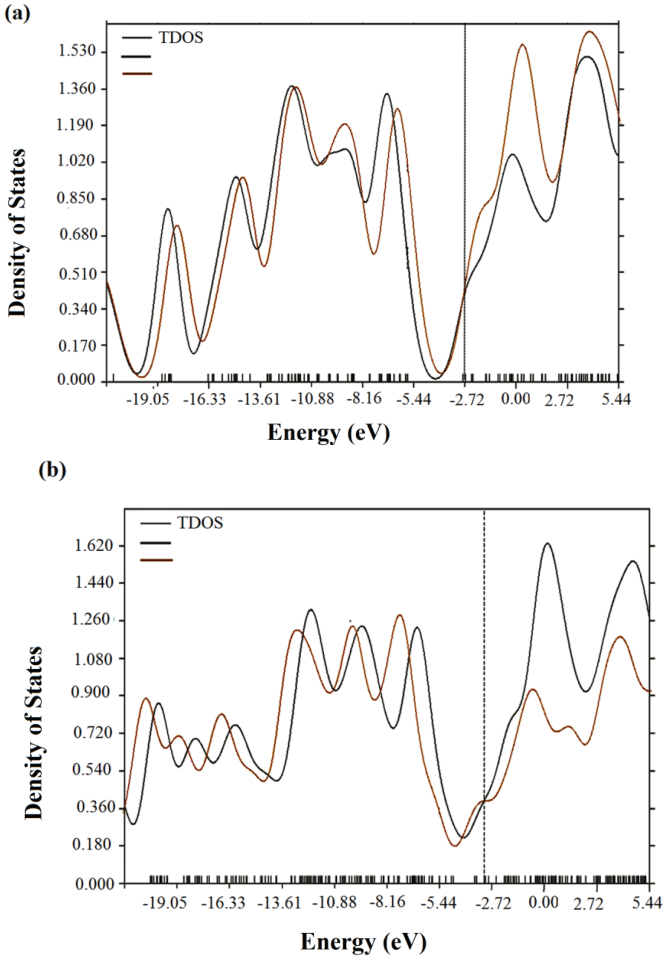

Fig. 2. Surface of density of state (DOS) of (a) BN-yne/BN-yne–Li and (b) GY/GY–Li.

The *DOS* plots indicate that the electronic properties are very sensitive to the Li adsorption, which would result in an electrical conductivity change of the decorated sheet according to the following equation:

$$\sigma = \exp\left(-E_g / 2kT\right) \tag{2}$$

where σ is the electric conductivity and k is the Boltzmann constant.[22] According to Eq. (2), smaller values of E_g at a given temperature lead to larger electric conductivity. Therefore, the predicted substantial decrement of E_g in Li-decorated GY and BN-yne upon Li adsorption induces a change in the electrical conductivity of these sheets. According to the obtained results, it could be seen that decorating these sheets with Li atoms alters their electronic and transport properties.

QTAIM analysis

QTAIM analysis can be used to connect the changes in charge of atoms in the molecules. Since the QTAIM method provides a major amount of information about the nature of bonding, the topological properties of the electron density, the Laplacian of the electron density, the total electronic energy density, the electronic kinetic energy density and the delocalization index, δ(A, B) were explored at various bond critical points (BCPs) to characterize the presence of possible open-shell and closed-shell interactions in the coordination sphere. The delocalization index provides a measure of the number of electrons shared or exchanged between two atoms connected by a bond path and could be interpreted as the bond order when charge-transfer between atoms A and B is not significant. QTAIM analysis was employed to elucidate the interactions between the Li atoms and GY and BN-yne. Based on the systematic analysis of the Li–bond strength (Δ_{com}) was suggested using the properties of the proton-donating bond. This is based on the geometrical and topological parameters of the Li bonds with A (A: C, N, H or B):[17]

$$\Delta_{com} = \sum_{i=1}^{n}\left[\frac{\left(r_{Li-A} - r^{0}_{Li-A}\right)}{r^{0}_{Li-A}}\right]_i^2 + \sum_{i=1}^{n}\left[\frac{\left(\rho^{0}_{Li-A} - \rho_{Li-A}\right)}{\rho^{0}_{Li-A}}\right]_i^2 + \sum_{i=1}^{n}\left[\frac{\left(\nabla^2\rho_{Li-A} - \nabla^2\rho^{0}_{Li-A}\right)}{\nabla^2\rho^{0}_{Li-A}}\right]_i^2 \quad (3)$$

where $r_{Li–A}$, $\rho_{Li–A}$, and $\nabla^2\rho_{Li–A}$ correspond to the proton-donating bond involved in Li bonding: the bond length, electronic density of Li–A bond critical point, and the Laplacian of this density, respectively. Similarly, $r^0_{Li–A}$, $\rho_{Li–A}$, and $\nabla^2\rho^0_{Li–A}$ correspond to the same parameters of the Li–A bond not involved in the Li–bond formation, the Δ_{com} values of decorated GY and BN-yne are 4.31 and 4.44, respectively.

As presented by Bader,[17] the strength of a chemical bond and its bond order (*BO*) are reflected in the electron density at the BCP:

$$BO = \exp[A(\rho_b - B)] \quad (4)$$

where A and B are constants that depend on the nature of the bonded atoms. Furthermore, $\delta(A,B)$ was calculated between bonded atoms and the bond order between them could be obtained if the electron pairs were equally shared. As ρ and the BO are strongly correlated (Eq. (4)), it was suggested calibrating this correlation using the delocalization index rather than arbitrarily assigned bond orders:

$$\Delta(A,B) = \exp[A(\rho_c - B)] \quad (5)$$

However, the relation between ρ and BO (Eq. (4)) could used to estimate the results of this work. As observed in Tables III and IV, the maximum values for the electron densities are related to c4 and c′4 in BN-yne and BN-yne–Li (0.3785 and 0.3697 a.u.), which show that the atoms in the bond have sp hybridization. In GY and GY–Li c3, c′3 have the maximum values (0.3848 and 0.3704 a.u.). The

TABLE III. Selected topological parameters of the investigated molecules and $Hc(r)$, $Gc(r)$ and $Vc(r)$. The density of the total energy of electrons related to B3LYP/6–31g(d) of BN-yne and BN-yne–Li

Parameter	$\rho_c(r)$[a] / a.u.	$\nabla^2\rho_c(r)$ [b] / a.u.	$H_c(r)$[c] / a.u.	$V_c(r)$[d] / a.u.	$G_c(r)$[e] / a.u.
BN-yne					
c1	0.16141	–0.13040	0.10456	–0.33954	0.23498
c2	0.18112	–0.14824	0.12752	–0.40327	0.27575
c3	0.30857	0.162058	0.34001	–0.51791	0.17795
c4	0.37854	0.258935	0.51951	–0.78021	0.26064
c5	0.18631	–0.02933	0.16938	–0.36809	0.19871
c6	0.16542	–0.13085	0.10976	–0.35036	0.24061
c7	0.16542	–0.13084	0.10976	–0.35037	0.24061
C8	0.01948	–0.02958	–0.00299	–0.02358	0.02658
C9	0.00282	–0.00310	–0.00075	–0.00159	0.00235
BN-yne–Li					
c'1	0.16707	–0.14227	0.10956	–0.36141	0.25184
c'2	0.16533	–0.16320	0.10279	–0.36871	0.26599
c'3	0.32169	0.14928	0.38650	–0.62372	0.23720
c'4	0.36974	0.25603	0.49084	–0.72566	0.23481
c'5	0.19476	–0.05709	0.18108	–0.41923	0.23810
c'6	0.15011	–0.12047	0.09369	–0.30785	0.21419
c'7	0.14851	–0.12508	0.09059	–0.30627	0.21568
c'8	0.01752	–0.03156	–0.00518	–0.02119	0.02637
c'9	0.01914	–0.03463	–0.00550	–0.02362	0.02912
c'10	0.02386	–0.04236	–0.00518	–0.03198	0.03717
c'11	0.02642	–0.04551	–0.00471	–0.03601	0.04076
c'12	0.02044	–0.03074	–0.00482	–0.02110	0.02593
c'13	0.02025	–0.02949	–0.00249	–0.02448	0.02698
c'14	0.01872	–0.02690	–0.00246	–0.02197	0.02443

[a]Electron density ($\rho_c(r)$); [b]Laplacian ($\nabla^2\rho_c(r)$); [c]total electronic energy density ($H_c(r)$); [d]electronic potential energy density ($V_c(r)$); [e]electronic kinetic energy density ($G_c(r)$)

TABLE IV. The selected topological parameters of the investigated molecules and the density of $H_c(r)$, $G_c(r)$ and $V_c(r)$ (in a.u.). The density of the total energy of electrons related to B3LYP/6–31g(d) of GY and GY–Li

Parameter	$\rho_c(r)$[a]/ a.u.	$\nabla^2\rho_c(r)$ [b]/ a.u.	$H_c(r)$[c]/ a.u.	$V_c(r)$[d]/ a.u.	$G_c(r)$[e] /a.u.
GY					
c1	0.29048	0.21038	0.3134	–0.41651	0.10306
c2	0.28334	0.20184	0.30006	–0.39828	0.09822
c3	0.38483	0.27152	0.49991	–0.72831	0.22839
c4	0.28395	0.20337	0.30122	–0.39906	0.09784
c5	0.28350	0.20292	0.30089	–0.39886	0.09797
c6	0.02204	–0.03150	–0.00454	–0.02240	0.02695
c7	0.02090	–0.02937	–0.00429	–0.02079	0.02508
GY–Li					
c'1	0.27422	0.18981	0.28542	–0.38104	0.09561
c'2	0.28357	0.19250	0.30195	–0.41140	0.10945
c'3	0.37041	0.26034	0.47036	–0.68038	0.21001
c'4	0.28467	0.19323	0.30398	–0.41472	0.11074
c'5	0.25818	0.17092	0.25748	–0.34404	0.08656
c'6	0.02254	–0.03734	–0.00488	–0.02758	0.03246
c'7	0.02116	–0.03451	–0.00474	–0.02501	0.02976
c'8	0.02065	–0.03376	–0.00468	–0.02439	0.02907
c'9	0.02206	–0.03633	–0.00499	–0.02633	0.03133
c'10	0.02027	–0.03350	–0.00485	–0.02380	0.02865
c'11	0.02245	–0.02882	–0.00277	–0.02327	0.02604

[a]Electron density ($\rho_c(r)$); [b]Laplacian ($\nabla^2\rho_c(r)$); [c]total electronic energy density ($H_c(r)$); [d]Electronic potential energy density ($V_c(r)$); [e]Electronic kinetic energy density ($G_c(r)$)

investigated critical points are (3,–1) and (3,+1). The (3,–1) point is a maximum ρ in the plane defined by the corresponding eigenvectors, but a minimum ρ along the third axis that is perpendicular to this plane while the (3, +1) point is a minimum ρ in the plane defined by the corresponding eigenvectors and a maximum along the third axis that is perpendicular to this plane. There are two other critical points, (3,–3) and (3,+3) where ρ is a local maximum and a local minimum, respectively. Each type of critical point described above is identified by an element of chemical structure: (3,–3) is a nuclear critical point (NCP), (3,–1) is a bond critical point (BCP), (3,+1) is a ring critical point (RCP) and (3,+3) is a cage critical point (CCP). The number and type of critical points that can co-exist in a molecule or crystal follow a strict topological relationship:

$$n_{\mathrm{NCP}} - n_{\mathrm{BCP}} + n_{\mathrm{RCP}} - n_{\mathrm{CCP}} = \begin{cases} 1 & (\text{Isolated molecules}) \\ 0 & (\text{Infinite crystals}) \end{cases} \quad (6)$$

where n denotes the number of the subscripted type of CP. The first equality is known as the Poincaré–Hopf relationship and applies to isolated finite systems, such as a sheet while the second equality is known as the Morse Equation and

applies in cases of infinite periodic lattices. The set (n_{NCP}, n_{BCP}, n_{RCP}, n_{CCP}) for a given system is known as the ''characteristic set''. The linking of the Li to GY and BN-yne atoms results in the formation of three-membered rings and a ring CP in the face of each ring, where the density attains its minimum value in the ring surface (Figs. 3 and 4). There is also a ring CP in the center of a ring, and this ring surface, together with the four surfaces formed by the links to the Li atom, define a cage enclosing a (3, +3) or cage CP. The results obtained in the topological analysis of electron density are summarized in Tables III and IV. For complexes of Li with GY and BN-yne, the values of electron density are in the range of 0.0113–0.3704 and 0.0028–0.3785, respectively.

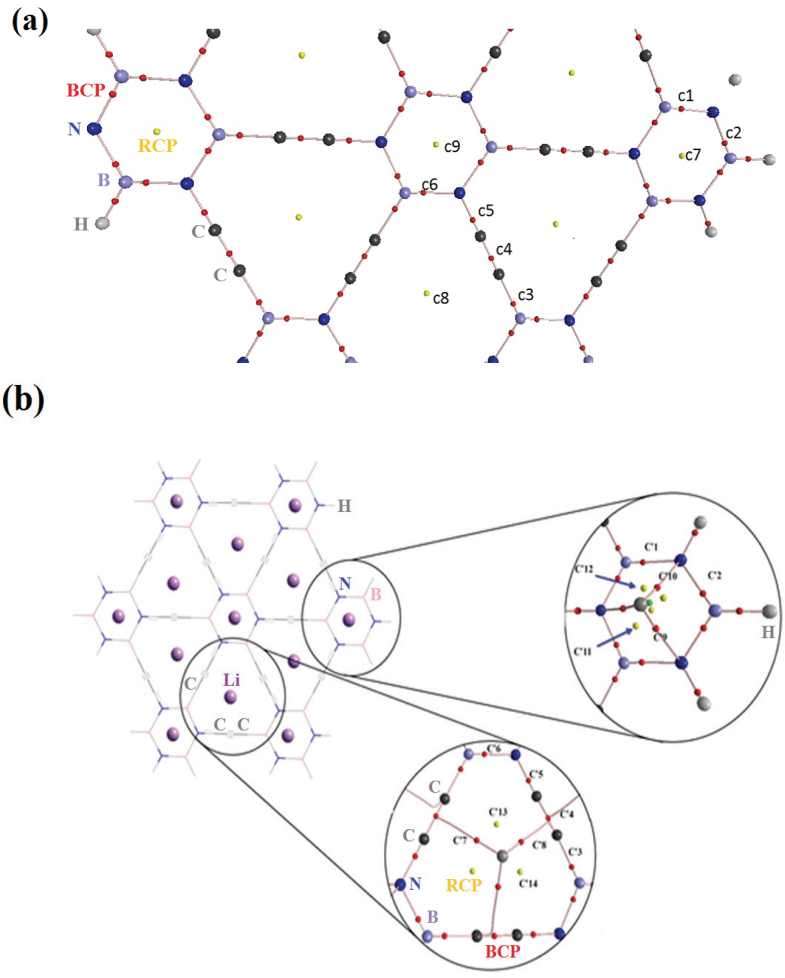

Fig. 3. Molecular graphs of a) BN-yne and b) BN-yne–Li obtained by QTAIM analysis. Bond critical points: red circles; ring critical points: yellow circles; bond paths: pink lines.

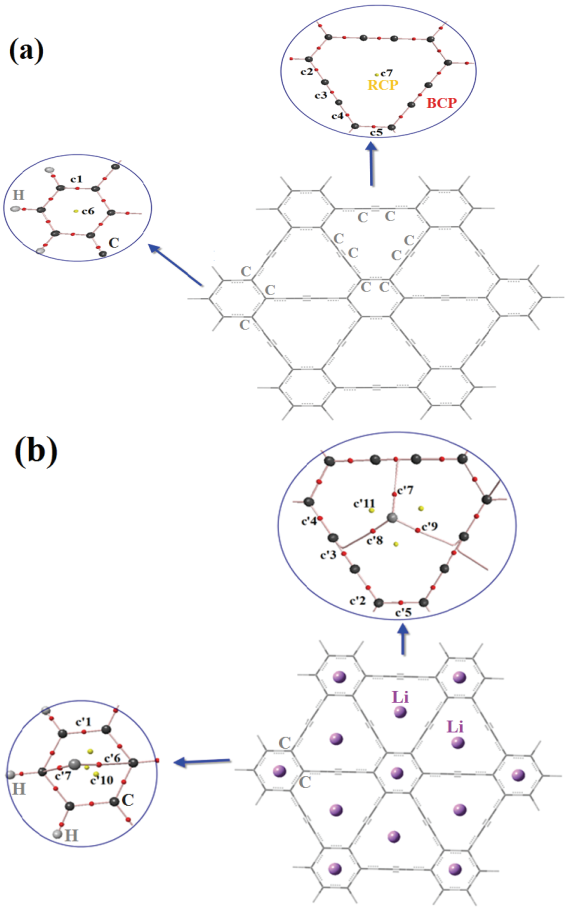

Fig. 4. Molecular graphs of: a) GY and b) GY–Li obtained by QTAIM analysis.

Molecular electrostatic potential (MEP)

The electron density is considered a very important factor in the understanding of the reactivity of electrophilic and nucleophilic sites and the interactions of hydrogen bonding.[23]

Thus, to predict this reactivity of attacks on the nucleophilic and electrophilic sites for the two compounds, the MEP of these compounds was simulated using the B3LYP level of the optimized geometry. The different colors red, blue and green represent the different regions at the MEP surface, *i.e.*, the most negative, the most positive, and zero electrostatic potential, respectively. The negative electrostatic potential at the MEP (shade of red) indicates that this is a region where a proton is attracted by the aggregate electron density in the molecule, while the positive electrostatic potential (shade of blue) is the region that is responsible for repulsion of a proton by the atomic nuclei. The negative region at MEP (red) corresponds to electrophilic reactivity (region of most electronegative

electrostatic potential) and the positive region (blue) corresponds to nucleophilic reactivity (region of the most positive electrostatic potential) and green represents region of zero potential. In Fig. 5, it should be emphasized that the maximum negative region having a positive potential is localized over the hollow sites. The contour map provides a simple way to predict how different geometries could interact. The contour maps of MEP are in good agreement with the other obtained results.

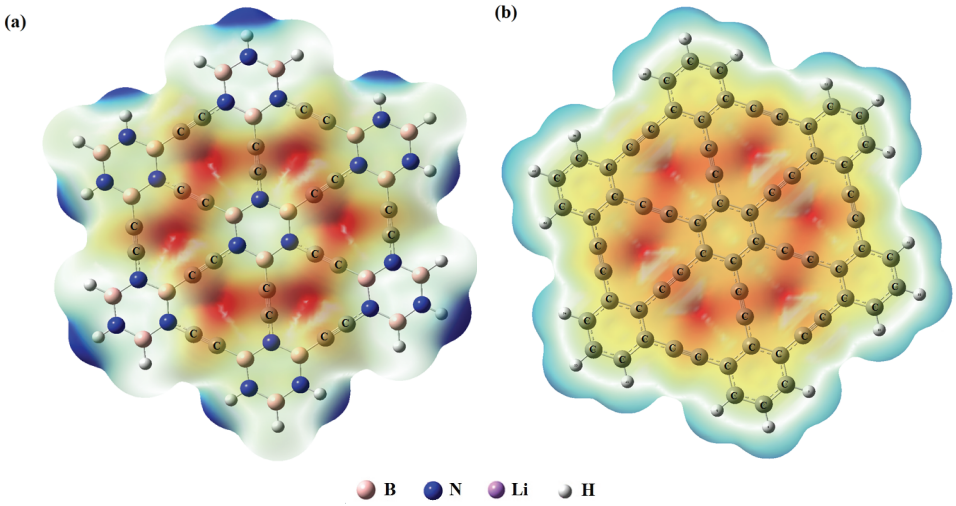

Fig. 5. Electron density surface maps with electrostatic potential surface for: a) BN-yne and b) GY.

CONCLUSIONS

The geometric structures and electronic properties of GY and BN-yne decorated with Li atoms were explored using DFT calculations. It was found that Li atoms could interact with these sheets. Indeed, the relationship between the interaction strength and the stability of the involved Li bonds was explored. A topological study of the electron density and its Laplacian at BCPs clearly demonstrated that the bond strength was in direct relationship with order bond. It is important to mention that this trend was also decorated *via* QTAIM charge analysis. In order to gain a more accurate insight into the nature of bonding interactions between Li and GY and BN-yne, recent QTAIM indicators were applied as quantitative evidence.

ИЗВОД

QTAIM ПРОУЧАВАЊЕ ДЕКОРИСАНОГ ГРАФИНА И БОР-НИТРИДА ЗА ДЕТЕКЦИЈУ Li

MARYAM DEHESTANI[1], LEILA ZEIDABADINEJAD[1,2] и SEDIGHEH POURESTARABADI[1,2]

[1]*Department of Chemistry, Shahid Bahonar University of Kerman, Kerman 76169, Iran и* [2]*Young Researchers Society, Shahid Bahonar University of Kerman, Kerman 76169, Iran*

Теоријом функционала густине истраживана је интеракција између тринаест атома Li са графином (GY) и са бор-нитридом (BN) као и молекулски електростатички потенцијал (MEP). Електронске и структурне особине интеракције између празних места на GY и BN са атомима Li представљене су у оквиру квантне теорије атома у молекулу (QTAIM). Теоријско разумевање интеракције атома Li и проширене мрежне структуре базиране на угљенику кључно је за развој нових материјала. Дат је извештај о израчунавању утицаја додавања Li на GY и BN. Предвиђено је да додавање Li повећава густину електронских стања у овим листовима. Због јаке интеракције између Li и GY и BN, опажене су јаке промене угљеничних листова упоредо са великим променама у енергетском процепу између трака. Ова студија баца јасно светло на хемијске особине нових, на угљенику базираних, 2D структура сложенијих од графинских листова.

(Примљено 25. јула, ревидирано 5. новембра, прихваћено 7. новембра 2016)

REFERENCES

1. K. S. Novoselov, A. K. Geim, S. Morozov, D. Jiang, Y. Zhang, S. A. Dubonos, I. Grigorieva, A. Firsov, *Science* **306** (2004) 666
2. A. K. Geim, K. S. Novoselov, *Nat. Mater.* **6** (2007) 183
3. A. Hirsch, *Nat. Mater.* **9** (2010) 868
4. R. J. Lagow, J. J. Kampa, H.-C. Wei, S. L. Battle, J. W. Genge, D. A. Laude, C. J. Harper, R. Bau, R. C. Stevens, J. F. Haw, *Science* **267** (1995) 362
5. W. A. Chalifoux, R. R. Tykwinski, *Nat. Chem.* **2** (2010) 967
6. S. Schrettl, C. Stefaniu, C. Schwieger, G. Pasche, E. Oveisi, Y. Fontana, *Nat. Chem.* **6** (2014) 468
7. Y. Li, L. Xu, H. Liu, Y. Li, *Chem. Soc. Rev.* **43** (2014) 2572
8. A. Ivanovskii, *Prog. Solid State Chem.* **41** (2013) 1
9. R. Baughman, H. Eckhardt, M. Kertesz, *J. Chem. Phys.* **87** (1987) 6687
10. N. Narita, S. Nagai, S. Suzuki, K. Nakao, *Phys. Rev., B* **58** (1998) 11009
11. M. M. Haley, *Pure Appl. Chem.* **80** (2008) 519
12. M. Long, L. Tang, D. Wang, Y. Li, Z. Shuai, *ACS Nano* **5** (2011) 2593
13. J. Zhou, K. Lv, Q. Wang, X. Chen, Q. Sun, P. Jena, *J. Chem. Phys.* **134** (2011) 174701
14. H. Zhang, M. Zhao, X. He, Z. Wang, X. Zhang, X. Liu, *J. Phys. Chem., C* **115** (2011) 8845
15. J. Kang, J. Li, F. Wu, S.-S. Li, J.-B. Xia, *J. Phys. Chem., C* **115** (2011) 20466
16. M. Frisch, G. Trucks, H. B. Schlegel, G. Scuseria, M. Robb, J. Cheeseman, G. Scalmani, V. Barone, B. Mennucci, G. Petersson, Gaussian 09, revision A. 02, Gaussian, Inc., Wallingford, CT, 2009)
17. R. F. W. Bader, *Atoms in molecules*, Wiley Online Library, 1990
18. R. Bader, AIM2000 Program, v. 2.0, McMaster University, Hamilton, ON, Canada, 2000
19. K. Fukui, T. Yonezawa, H. Shingu, *J. Chem. Phys.* **20** (1952) 722
20. K. Fukui, T. Yonezawa, C. Nagata, H. Shingu, *J. Chem. Phys.* **22** (1954) 1433
21. A. E. Reed, L. A. Curtiss, F. Weinhold, *Chem. Rev.* **88** (1988) 899
22. S. M. Sze, K. K. Ng. *Physics of semiconductor devices*, 3rd ed., Wiley, New York, 2006
23. E. E. Hodgkin, W. G. Richards, *Int. J. Quant. Chem.* **32** (1987) 105.